

## Article

# Danger Zone for Paramedian Forehead Flap Elevation: Maximizing Flap Length and Viability

Kylie A. Limback<sup>1</sup>, Alyssa H. Kendell<sup>1</sup>, Micaela Motzko<sup>1</sup>, Christopher C. Surek<sup>2</sup> and Jennifer F. Dennis<sup>2,\*</sup> <sup>1</sup> College of Osteopathic Medicine, Kansas City University, Kansas City, MO 64106, USA<sup>2</sup> Department of Pathology & Anatomical Sciences, Kansas City University, Kansas City, MO 64106, USA

\* Correspondence: jenniferdennis816@gmail.com; Tel.: +1-816-654-7536

**Abstract:** The supratrochlear artery (STA) demonstrates anatomical variability that impacts facial reconstruction with a paramedian forehead flap. STA branching patterns and the distance to the midline have been reported, but the STA pedicle has not been characterized. Our aim was to triangulate the STA pedicle relative to known anatomical landmarks and identify a danger zone to aid surgeons in creating viable tissue flaps. The upper facial region was dissected bilaterally on 38 cadaveric donors. Measurements from the supraorbital neurovascular bundle, orbital rim, and medial canthus to the STA pedicle were collected. Data were tallied and statistically analyzed. Measurement means, range, and standard deviations were calculated; no significant differences were found in the laterality of the measurements ( $p > 0.05$ ). Statistically significant, sex-based differences were identified for all measurements collected among male and female donors. This study characterizes a surgical danger zone for the STA pedicle specific to a paramedian forehead flap and identifies important differences within this danger zone among male versus female donors that surgeons should consider to prevent pedicle violation and enhance surgical success while maximizing flap length and mobility.

**Keywords:** paramedian forehead flap; supratrochlear artery; danger zone; surgery; facial surgery; ophthalmic artery



**Citation:** Limback, K.A.; Kendell, A.H.; Motzko, M.; Surek, C.C.; Dennis, J.F. Danger Zone for Paramedian Forehead Flap Elevation: Maximizing Flap Length and Viability. *Surgeries* **2024**, *5*, 13–23. <https://doi.org/10.3390/surgeries5010004>

Academic Editor: Cornelis F. M. Sier

Received: 1 December 2023

Revised: 3 January 2024

Accepted: 9 January 2024

Published: 11 January 2024



**Copyright:** © 2024 by the authors. Licensee MDPI, Basel, Switzerland. This article is an open access article distributed under the terms and conditions of the Creative Commons Attribution (CC BY) license (<https://creativecommons.org/licenses/by/4.0/>).

## 1. Introduction

The blood supply of the face is complex and made singular through anastomotic terminal blood sources. The forehead is primarily supplied by two terminal branches of the ophthalmic artery [1,2]: the supraorbital and supratrochlear (STA) arteries. Due to its role in reconstructive facial surgery, a thorough understanding of the STA course through forehead tissue planes allows surgeons to better protect the STA pedicle, dissecting the appropriate musculature both medial and lateral to the artery. The STA has an average diameter of approximately 1.00 mm [3–5], an average depth from the epidermal surface of 1.50 mm, and an average length from the occipital artery branch point to crossing the supraorbital rim of 51.1 mm [6]. The STA pierces the orbital septum 1.70–2.20 cm from the midline and ascends in the paramedian position 1.50–2.00 cm from the midline on average [2]. Indeed, extensive evaluation of the branching patterns of the STA has revealed an intricate system of vascular anastomoses in the nasoglabellar area, with contributions from the angular artery, the terminal facial artery, the supraorbital artery, the STA, and their respective contralateral vessels [1–3,7]. As this vascular arcade contains branches from both the internal and external carotid arteries, the possibility of retrograde blood flow through these anastomotic channels may be maintained through a variety of vascular medical complications [2–4].

Reconstruction of facial defects is a complex process that challenges surgeons to maintain facial characteristics while addressing clinical concerns. Mid-facial reconstruction of moderate facial defects incorporates the use of regional flaps, defined as donor tissue

pedunculated with a blood supply, but which do not need to be immediately adjacent to the reconstruction site. Recent cataloging of techniques utilized to repair the midfacial region identified 12 different flaps as the most common techniques for the midfacial region: the bilobed flap, the rhomboid flap, facial artery-based flaps (nasolabial flap, island composite nasal flap, and retroangular flap), the cervicofacial flap, the paramedian forehead flap, the frontal hairline island flap, the keystone flap, the Karapandzic flap, the Abbé flap, and the Mustardé flap [5]. The 12 flaps can be further divided into the type of flap (rotational, transpositional, advancement, or combination) as well as the specific midfacial region (upper lip, nose, cheek, etc.). [5]. Of these 12 options, the paramedian forehead flap is a rotational flap primarily utilized to treat nasal defects [5–9]. Paramedian forehead flaps have several advantages, including the ability to supply a large amount of tissue, the creation of a reliable flap, and minimal donor site morbidity [5–10]. The paramedian forehead flap is typically performed as a two- or three-stage procedure [11], requiring additional surgeries to divide the vascular pedicle and further construct the transplanted flap to resemble the native structure. Contralateral flaps are routinely used as they provide a decreased risk of kinking the pedicle and thereby disrupting the vascular supply; however, the constructed flap must then be longer to reach the targeted area. In order to effectively create and elevate the paramedian forehead flap, most surgeons adhere to a specific order of operative steps to ensure flap success (Figure 1). Pedicle division is performed three to four weeks postoperatively, allowing sufficient time for neovascularization [10–12]. The pedicle base defect is then closed. Additional flap thinning and sculpting revisions to better mirror adjacent structures and improve aesthetic outcomes may be considered.

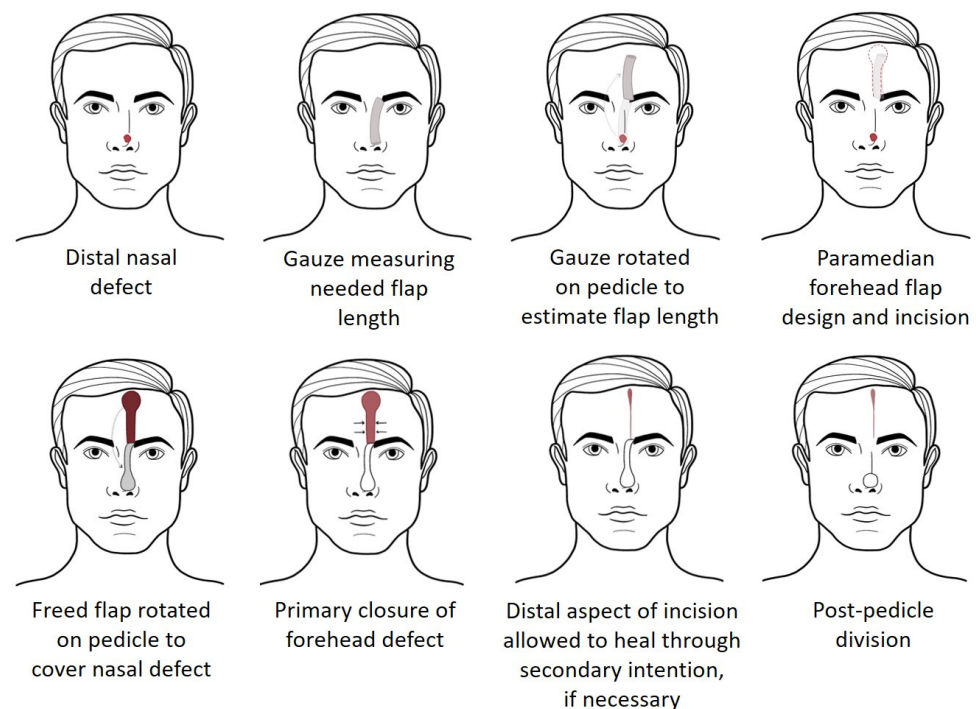


**Figure 1.** Paramedian forehead flap procedure steps, with step progression from left to right and top to bottom. The nasal defect is identified and cleaned, and healthy tissue margins are created. A template is created using flexible material (gauze) from the defect to the contralateral pedicle base. The template is rotated medially to the face axially to approximate the flap length. An incision is made along template borders, and tissue is lifted distal to proximal, leaving the pedicle intact. The flap is rotated on the pedicle to reach the defect, with primary closure of the forehead incision. Post-pedicle division to be pursued as needed on a specific patient basis. Surgical approach and image adapted from Mellette et al. (8 pictures) [11] and Correa et al. (9 steps) [12].

Though the literature has established that the STA ascends the forehead 1.50–2.00 cm from the facial midline [2], no other surface landmarks have been found that provide additional information as to the position of the STA. This paucity in the literature widens further when attempting to identify the STA pedicle, which is essential to avoid flap ischemia, necrosis, and flap failure. Reece et al. suggested preserving seven mm of uninterrupted tissue above the supraorbital rim to maintain vascular safety, based on measurements from five cadaveric heads [13]. This study greatly expands these measurements and characterizes additional anatomical landmarks for utilization during the design and execution of paramedian forehead flaps to decrease vascular compromise and improve postoperative outcomes.

## 2. Materials and Methods

### 2.1. Cadaveric Donors

Thirty-eight cadavers, both whole-body and decapitated donors, from the Gift Body Program at Kansas City University (KCU) and the Deeded Body Program University of Nebraska Medical Center were utilized (Institutional Biosafety Committee, #1819182-1). The 35 whole-body donors were formalin-embalmed, with the remaining three cadavers being frozen-fresh head donors. The cadavers were unable to be injected with latex due to embalming and restrictions associated with the body donation agreement. The dissections were performed bilaterally, with unilateral dissections taking place only in the setting of contralateral side compromise ( $n = 4$ ), for a total of 72 individual pedicles used for measurements. The right and left STA pedicle measurements of each donor were categorized as individual specimens and recorded. Additional demographics recorded included sex, age, weight, and height.

### 2.2. Dissection Approach

The anatomical landmarks used to localize the STA pedicle origin were the bony orbital rim, supraorbital neurovascular bundle, and medial canthus. To triangulate a danger zone surrounding the STA pedicle, measurements from the supraorbital neurovascular bundle, bony orbital rim, and medial canthus to the STA flap pedicle were obtained bilaterally using a digital caliper (General Ultratech, San Jose, CA, USA). The facial midline to the STA pedicle, a standard that has been previously described as 1.50–2.00 cm, was also measured to serve as a control [2].

All cadavers were placed in the supine position, with the researcher performing all methods standing at the cranial aspect of the dissection table to replicate surgical positioning. Before dissection, all specimens were measured and marked to construct a pre-dissection diagram for creating a paramedian forehead flap such as in the operation room (Figure 2). A singular dotted line was drawn on the facial midline (using the nasal septum, philtrum, and chin cleft when present to visualize the midline) to use for further measurements. Bilateral markings consisted of measuring 1.70 cm from the facial midline to approximate the location of the ascending STA. Then, measurements of 0.70 cm both medial and lateral to the STA mark were made to visualize the flap width. The last two marks were continued from the eyebrow to the hairline to create the potential flap length. A final mark was measured 2.50 cm from the midline for the creation of a second flap to assist in localizing the supraorbital neurovascular bundle. This wide marker allowed dissection without accidental disruption of the supraorbital neurovascular bundle past the supraorbital margin transition point. All measurements and markings were performed bilaterally on all cadaveric specimens before dissection by the first author with the same digital caliper to maintain consistency and limit potential variations.



**Figure 2.** Pre-dissection diagram and measurements. The black mark is the facial midline. The blue mark is 1.70 cm from the midline, marking the average STA location. The red mark is 0.70 cm from either side of the blue mark, creating the flap width. The green mark is 2.50 cm from the midline, marking the average supraorbital neurovascular bundle location.

### 2.3. Measurement of STA Pedicle to Anatomical Landmarks

After the creation of the paramedian forehead flap, a #10 scalpel blade was used to trace the flap design, cutting through all five scalp layers. After freeing the flap, forceps were used to carefully lift the tissue flap and allow visualization of the periosteum. The periosteum was then elevated using a freer elevator, starting the cephalad and moving the caudad (Figure 3A). As the STA pedicle was approached, dissecting movements were minimized to not disrupt the origin of the pedicle. Once the pedicle was adequately visualized, its origin was marked. The first author then used a digital caliper to measure from the facial midline to the pedicle marking (Figure 3B). Then, the pedicle was disrupted with the further freeing of the paramedian forehead flap. Once the flap was retracted fully, the measurement from the STA pedicle marking to the medial canthus was recorded (Figure 3C). Due to the flap thickness on some specimens, the flap was completely removed with a #10 scalpel blade when it interfered with medial canthus to pedicle measurements. A vertical incision was made from the 2.50 cm mark approximately halfway up the forehead; this cut was connected to the lateral flap cut with a small horizontal incision in the middle of the forehead. After freeing the second constructed flap, forceps were used to lift the tissue flap and allow visualization of the periosteum. The periosteum was then elevated using a freer elevator, starting with the cephalad and moving toward the caudad (Figure 3D). After locating the supraorbital neurovascular bundle, a measurement was taken from its origin to the STA pedicle marking (Figure 3E). Though the supraorbital neurovascular bundle is not visualized clinically, this marker was included to confirm the pedicle position. Finally,

all remaining supraorbital tissue was lifted with forceps and a freer elevator to visualize the bony orbital rim. The most direct measurement from the bony orbital rim to the pedicle marking was then recorded (Figure 3F).

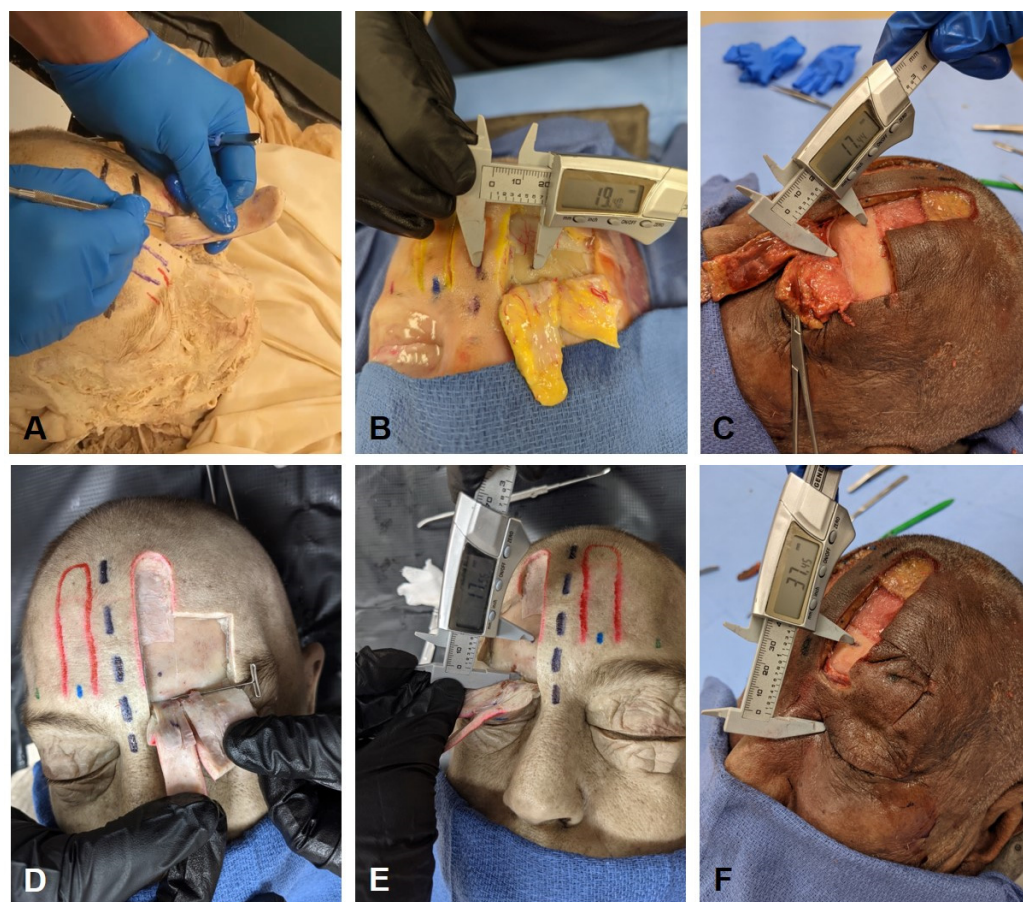


**Figure 3.** Measurements from the STA pedicle to anatomic landmarks. (A) Elevating the periosteum with the freer elevator. (B) STA pedicle to the facial midline. (C) STA pedicle to the medial canthus. (D) Visualization of the supraorbital neurovascular bundle. (E) STA pedicle to the supraorbital neurovascular bundle. (F) STA pedicle to the bony orbital rim.

#### 2.4. Statistical Analysis

Data were tallied and analyzed using Excel (Microsoft, Takoma, WA, USA). An independent sample *t*-test was used for all four variables to determine the significance between the mean of the right- and left-sided measurements and the anatomical sex of the cadavers. A Mann–Whitney U test was used to evaluate differences in the means of embalmed vs. fresh cadavers due to differences in sample size using SPSS (Statistical Product and Service Solutions, IBM, Armonk, NY, USA). An intraclass correlation coefficient was not performed as all measurements were conducted by the first author. Significance was set at  $p < 0.05$ . All data are expressed as the mean  $\pm$  standard error of the mean, with the range included.

### 3. Results

Thirty-eight cadavers were utilized for this study, with a total of 72 pedicles dissected and measured. Of these, three cadavers were fresh with a total dissection of six samples, and thirty-five cadavers were embalmed with a total dissection of sixty-seven pedicles. Of the 38 cadavers, 20 were male and 18 were female, with a mean age of 75.2 years, ranging from 44 to 103 years old. The means, standard deviations, and ranges for each measurement were calculated and documented.

### 3.1. Facial Midline to the STA Pedicle

The mean measurement for the facial midline to the STA pedicle was 1.69 cm (std. dev., 0.14; range, 1.30–2.00 cm). In right- versus left-sided measurements, there were no significant differences ( $p > 0.05$ ) between the distance of the STA pedicle to the facial midline; however, a significant difference was found between males and females (Table 1). Additionally, a significant difference was found between fully intact embalmed cadavers and fresh-head cadavers (Table 1).

**Table 1.** All measurements taken in centimeters (cm = centimeter); STA = supratrochlear artery; total cadavers,  $n = 72$  samples (male,  $n = 39$ ; female,  $n = 33$ ); fresh cadaver,  $n = 3$  (6 samples); formalin-embalmed cadavers,  $n = 35$  (67 samples); \*\* a Mann–Whitney U test was used to evaluate differences in the means of embalmed vs. fresh cadavers; \* an independent sample  $t$ -test was used to determine the significance between male and female cadavers.

Formalin-Embalmed Cadavers versus Fresh Disarticulated Head and Neck Cadavers			
	Embalmed Cadaver Mean $\pm$ SD	Fresh Cadaver Mean $\pm$ SD	$p$ -value *
Facial Midline to the STA Pedicle	1.68 $\pm$ 0.14	1.81 $\pm$ 0.10	<0.05
Supraorbital Neurovascular Bundle to the STA Pedicle	1.48 $\pm$ 0.33	1.73 $\pm$ 0.73	0.265
Bony Orbital Rim to the STA Pedicle	1.54 $\pm$ 0.37	1.52 $\pm$ 0.56	0.684
Medial Canthus to the STA Pedicle	3.04 $\pm$ 0.36	3.23 $\pm$ 0.51	0.283
STA Measurements in Male versus Female Cadavers			
	Male Cadaver Mean $\pm$ SD	Female Cadaver Mean $\pm$ SD	$p$ -value **
Facial Midline to the STA Pedicle	1.75 $\pm$ 0.11	1.63 $\pm$ 0.16	<0.05
Supraorbital Neurovascular Bundle to the STA Pedicle	1.58 $\pm$ 0.37	1.40 $\pm$ 0.36	<0.05
Bony Orbital Rim to the STA Pedicle	1.65 $\pm$ 0.39	1.42 $\pm$ 0.35	<0.05
Medial Canthus to the STA Pedicle	3.17 $\pm$ 0.39	2.92 $\pm$ 0.31	<0.05

### 3.2. Supraorbital Neurovascular Bundle to the STA Pedicle

The mean measurement for the supraorbital neurovascular bundle to the STA pedicle was 1.50 cm (std. dev., 0.37; range, 0.60–2.70 cm). In right- versus left-sided measurements, there were no significant differences between the distance of the STA pedicle to the supraorbital neurovascular bundle. A significant difference was found between males and females (Table 1). No significant difference was found between fully intact embalmed cadavers and fresh-head cadavers (Table 1).

### 3.3. Bony Orbital Rim to the STA Pedicle

The mean measurement for the bony orbital rim to the STA pedicle was 1.53 cm (std. dev., 0.38; range, 0.60–2.20 cm). In right- versus left-sided measurements, there were no significant differences between the distance of the STA pedicle to the orbital rim. A significant difference was found between males and females (Table 1). No significant difference was found between fully intact embalmed cadavers and fresh-head cadavers (Table 1).

### 3.4. Medial Canthus to the STA Pedicle

The mean measurement for the medial canthus to the STA pedicle was 3.05 cm (std. dev., 0.37; range, 2.30–3.80 cm). In right- versus left-sided measurements, there were no significant differences between the distance of the STA pedicle to the medial canthus. A significant difference was found between males and females (Table 1). No significant

difference was found between fully intact embalmed cadavers and fresh-head cadavers (Table 1).

#### 4. Discussion

The STA represents a relatively small vessel with a short and constant course. It contributes to the rich anastomotic vascular plexus formed between itself, the supraorbital artery, the angular artery, and the terminal facial artery [1–3,14] to serve as the main contributors to the scalp's blood supply, supporting all five layers of the forehead. The STA traverses through these tissue layers, including the periosteum of the vault cranial bones, loose connective tissue, epicranial aponeurosis, dense subcutaneous connective tissue, and skin [14–16], as it ascends the medial forehead.

Considerable research has been performed to evaluate the branching pattern variations of the STA and the vascular arcade of the forehead and consistently cites the paramedian position of the STA as 1.50–2.00 cm [2]. However, the location of the STA pedicle from the midline and additional surgical anatomic landmarks has yet to be elucidated. The objective of this research study was to identify supplementary markers for reconstructive surgeons to utilize during the creation of paramedian forehead flaps to aid in minimizing damage to the vascular supply of the flap and subsequent surgical consequences. With these findings, a surgical dissection danger zone for the STA pedicle was established (Figure 4), which depicts the STA pedicle pathway as it ascends the forehead relative to external or palpable anatomical landmarks and represents where reconstructive surgeons should dissect with caution.

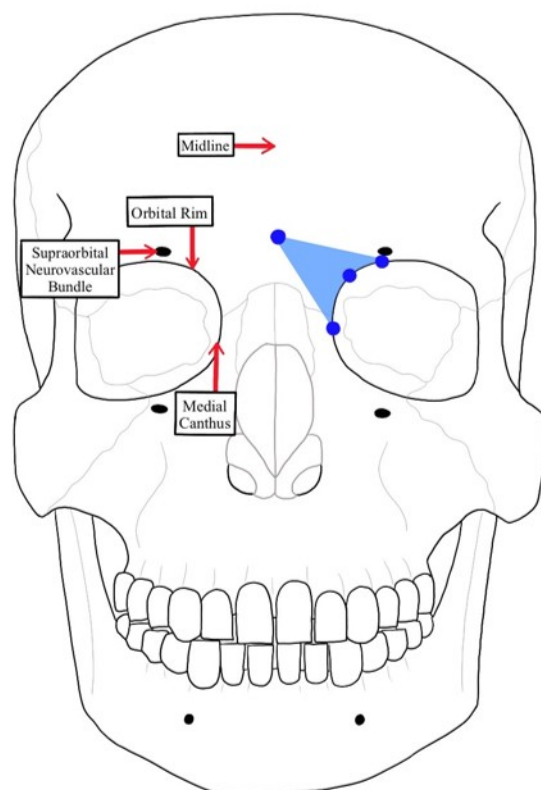


**Figure 4.** Surgical dissection danger zone. Graphic of the STA pedicle danger zone (blue triangle), which connects the external or palpable anatomical landmarks (blue dots) and represents the region where reconstructive surgeons should dissect with caution (shaded triangle).

All four measurements taken in this study were measured by the first author, supporting the reliability of the measurements by eliminating variations in measurement techniques and reducing the possibility of human error. Our findings of the STA pedicle to facial midline across the 72 samples largely support Shumrick and Smith's anatomical

studies [2], finding the average location of the pedicle to be 1.69 cm from the midline. However, the range from this study expands past the 1.50–2.00 cm listed previously, as 1.30–2.00 cm, highlighting the importance of soft surgical dissection on the medial aspect of the paramedian forehead flap.

There were no significant differences in right- versus left-sided measurements from all four anatomical points, demonstrating the consistent path of the STA as it supplies the surrounding tissues and ascends the forehead, regardless of the side. Significant differences were found in two of the four measurements between formalin-embalmed cadavers and fresh, disarticulated head and neck cadavers (Table 1). These findings may be explained by the embalming process and tissue fixation changing the relative positions of anatomical structures. However, this potential explanation is limited by the small sample size of fresh cadavers versus the larger sample size of embalmed cadavers, as well as the compounding factor of all fresh cadavers utilized being disarticulated heads and necks, while all embalmed cadavers were fully intact. The measurements that exhibited statistical significance are most likely due to the aforementioned small sample size, as previous studies have shown that there is not a notable difference between fresh tissue and embalmed tissue [17].

Statistical significance was also found for all measurements obtained between male and female cadavers (Table 1). In conjunction with the lack of statistical differences between right- and left-sided measurements, this finding highlights the importance of careful medical dissections, as all female measurement means were shorter than their male counterparts. This finding is not particularly unexpected as sex-based differences in facial characteristics have been previously studied and are commonly understood. In general, it is known that an individual's facial structure is influenced by a variety of factors, one of which is the person's sex [18]. A typical male's face is wider and longer with a more prominent brow structure and a more rectangular shape overall. In contrast, a typical female's face carries a rounder shape with less angulated facial features. With this knowledge established and accepted, it is further confirmed by the statistical differences found in male versus female measurements within this study. This finding is of particular significance due to the previously established reference range of 1.50–2.00 cm found by Shumrick and Smith, which was determined in a sample size of five cadavers [2]. In comparison, our evaluation of 72 hemifaces drastically expands the sample size as well as expands the reference range to 1.30–2.00 cm.

Paramedian forehead flaps remain a desirable surgical option for plastic and maxillofacial surgeons reconstructing nasal defects, commonly after the resection of nasal neoplasms [5,6]. Although flap dissection initially leaves an apparent forehead defect, resolution occurs through successive tissue remodeling and leaves overall cosmetic outcomes that are viewed positively by both the patient and surgeon [19]. Paramedian forehead flaps provide several other advantages, including providing ample tissue to cover large defects, and can be used to correct congenital [20] or acquired lesions [9,21,22]. Additionally, the paramedian forehead flap can be reused to repair remnant defects [23,24], as well as having the inherent flexibility to be modified by reconstructive surgeons to best suit individualized, patient-specific midfacial features [8,22,25]. Most importantly, these flaps, when dissected and implemented correctly, are associated with positive long-term outcomes [9].

As with any procedure, the paramedian forehead flap poses a variety of post-surgical risks. Minor complications include infection, partial nasal collapse, incomplete nasal obstruction, epidermolysis, and alar asymmetry [6,21,26–28]. Major complications include flap necrosis (both full and partial), nasal obstruction, alar notching, and asymmetry. The incidence of post-surgical complications has varied widely across reports. Little et al. found that 16.1% of patients developed a major complication during their postoperative course. Of these, patients exhibited flap necrosis (5.4%), nasal obstruction (4.9%), and alar notching (9.8%) [27]. Patients with necrotic flaps were further categorized as <50% or >50% necrosis, with <50% in nine patients and >50% in two. However, Chen et al. describe major complication indices of 31.7% and minor complication rates of 50.8%, with the most common

complications being infection (2.9%), bleeding (1.4%), and DVT (<0.5%) [29]. Collectively, these data are intermittently consistent with reports of infection (2.7%), bleeding (8.1%), and partial flap loss (2.7%) from Rajan et al. [20]. Though increased age and smoking are well-established risk factors for a wide variety of medical and postoperative complications, they have not been associated with statistically significant increases in negative outcomes in paramedian forehead flaps [30]. Paramedian forehead flap necrosis is a particularly serious complication, as it can lead to flap failure. By its nature, the vertical methodology of constructing a paramedian forehead flap creates the isolation of a single blood supply by the STA for the majority of the length of the tissue flap. Therefore, complications to the supratrochlear artery's blood supply can directly lead to flap necrosis and potential flap failure. Indeed, for patients with high vascular risk, a three-staged approach has been reported as a better functional and aesthetic option as compared to the typical two-staged approach [26].

Accurately identifying the anatomic location of the STA pedicle is a vital skill when performing paramedian forehead flap reconstruction. Though certainly, not all paramedian forehead flaps require maximal flap length to reach the defect, a subset of flaps may necessitate this additional length, particularly those located on the nasal tip or columella. As skin cancer continues to be the most diagnosed cancer in the United States [31], it remains essential for surgeons to be proficient at constructing paramedian forehead flaps, particularly in cases with delayed diagnoses and more invasive defects. The vertical design of the paramedian forehead flap eliminates all collateral blood supply and relies solely on the STA for vascular viability. With a thorough knowledge of approximate STA pedicle location, a reconstructive surgeon can more accurately isolate the pedicle, allowing for an optimal flap length while limiting the potential of flap compromise and failure.

Several considerations should be considered in future research on the STA pedicle location. Primarily, it must be noted that a majority of the donors were Caucasian, which limited the racial and ethnic diversity of the sample. Caution must be taken when projecting generalizations from this research across a wide variety of ethnic backgrounds. This study was also limited by the small sample size of fresh head and neck specimens. Further studies could be conducted utilizing only fresh cadaveric material for comparison. Future studies may also assess the presence and distance from the same or other anatomical landmarks to contribute to the body of evidence for safe dissection in paramedian forehead flaps.

## 5. Conclusions

This study highlights the importance of a thorough understanding of the exact anatomic location of the STA pedicle through careful dissection of surrounding relevant anatomical landmarks as it pertains to the creation and elevation of a paramedian forehead flap. The data reported in this study provide an STA pedicle danger zone to aid facial reconstructive surgeons in repairing nasal defects with greater success and less disruption of the vascular supply. We discovered a significant difference in all measurements obtained from male versus female donors. Overall, this study contributes novel information to the body of literature surrounding the STA pedicle and its relevance to the success of paramedian forehead flap surgery.

**Author Contributions:** Conceptualization, K.A.L. and C.C.S. methodology, K.A.L., C.C.S. and J.F.D.; validation, J.F.D.; formal analysis, K.A.L., A.H.K. and J.F.D.; investigation, K.A.L., A.H.K. and J.F.D.; data curation, K.A.L. and A.H.K.; writing—original draft preparation, K.A.L.; writing—review and editing, K.A.L., A.H.K., M.M., C.C.S. and J.F.D.; visualization, M.M.; supervision, J.F.D.; project administration, J.F.D. All authors have read and agreed to the published version of the manuscript.

**Funding:** This research received no external funding.

**Institutional Review Board Statement:** The cadaveric study protocol was approved by the Institutional Biosafety Committee of Kansas City University (1819182-1).

**Informed Consent Statement:** Informed consent, including permission to publish images for research and/or educational purposes, was obtained from all subjects involved in the study through their participation in the Gift Body Program at Kansas City University and the Deeded Body Program University of Nebraska Medical Center.

**Data Availability Statement:** Data are contained within the article.

**Acknowledgments:** The authors would like to express gratitude to the donors and their families for their invaluable contribution to the Gift Body Program at Kansas City University and the Deeded Body Program at the University of Nebraska Medical Center. Without their donations, the educational experiences of all students and fellows would not be what it is today.

**Conflicts of Interest:** Christopher Surek is a consultant for Allergan, Galderma, Revance, and Cypris Medical; all other authors have no disclosures to report.

## References

1. Dalley, A.F.I.A.; Anne, M.R. *Moore's Clinically Oriented Anatomy*, 9th ed.; Wolters Kluwer: Philadelphia, PA, USA, 2022.
2. Shumrick, K.A.; Smith, T.L. The anatomic basis for the design of forehead flaps in nasal reconstruction. *Arch. Otolaryngol. Head Neck Surg.* **1992**, *118*, 373–379. [[CrossRef](#)]
3. Yu, D.; Weng, R.; Wang, H.; Mu, X.; Li, Q. Anatomical study of forehead flap with its pedicle based on cutaneous branch of supratrochlear artery and its application in nasal reconstruction. *Ann. Plast. Surg.* **2010**, *65*, 183–187. [[CrossRef](#)]
4. Kelly, C.P.; Yavuzer, R.; Keskin, M.; Bradford, M.; Govila, L.; Jackson, I.T. Functional anastomotic relationship between the supratrochlear and facial arteries: An anatomical study. *Plast. Reconstr. Surg.* **2008**, *121*, 458–465. [[CrossRef](#)]
5. Salzano, G.; Maffia, F.; Vaira, L.A.; Committeri, U.; Copelli, C.; Maglitto, F.; Manfuso, A.; Abbate, V.; Bonavolontà, P.; Scarpa, A.; et al. Locoregional Flaps for the Reconstruction of Midface Skin Defects: A Collection of Key Surgical Techniques. *Clin. Med.* **2023**, *12*, 3700. [[CrossRef](#)]
6. Hammer, D.; Williams, F.; Kim, R. Paramedian Forehead Flap. *Oral Maxillofac. Surg. Clin.* **2020**, *28*, 23–28. [[CrossRef](#)]
7. Menick, F.J. A 10-year experience in nasal reconstruction with the three-stage forehead flap. *Plast. Reconstr. Surg.* **2002**, *109*, 1839–1855, discussion 1856–1861. [[CrossRef](#)]
8. Shokri, T.; Kadakia, S.; Saman, M.; Habal, M.B.; Kohlert, S.; Sokoya, M.; Ducic, Y.; Wood-Smith, D. The Paramedian Forehead Flap for Nasal Reconstruction: From Antiquity to Present. *J. Craniofacial Surg.* **2019**, *30*, 330–333. [[CrossRef](#)]
9. Apaydin, F.; Kaya, I.; Uslu, M.; Berber, V. Paramedia Forehead Flap in Large Nasal Skin Defects: Twenty-years' Experience. *Turk. Arch. Otorhinolaryngol.* **2022**, *60*, 155–160. [[CrossRef](#)]
10. Care UoI. Iowa Head and Neck Protocols: Paramedian Forehead Flap. University of Iowa. 2022. Available online: <https://medicine.uiowa.edu/iowaprotocols/paramedian-forehead-flap> (accessed on 1 December 2023).
11. Mellette, J.R.; Ho, D.Q. Interpolation flaps. *Dermatol. Clin.* **2005**, *23*, 87–112. [[CrossRef](#)]
12. Correa, B.J.; Weathers, W.M.; Wolfswinkel, E.M.; Thornton, J.F. The forehead flap: The gold standard of nasal soft tissue reconstruction. *Semin. Plast. Surg.* **2013**, *27*, 96–103. [[CrossRef](#)]
13. Reece, E.M.; Schaverien, M.; Rohrich, R. The paramedian forehead flap: A dynamic anatomical vascular study verifying safety and clinical implications. *Plast. Reconstr. Surg.* **2008**, *121*, 1956–1963. [[CrossRef](#)]
14. Gilroy, A.; MacPherson, B.; Wikenheiser, J.; Schunke, M.; Schulte, E.; Schumacher, U.; Voll, M.; Wesker, K. *Atlas of Anatomy*, 4th ed.; Thieme: New York, NY, USA, 2020.
15. Erdogmus, S.; Govsa, F. Anatomy of the supraorbital region and the evaluation of it for the reconstruction of facial defects. *J. Craniofacial Surg.* **2007**, *18*, 104–112. [[CrossRef](#)] [[PubMed](#)]
16. Detton, A.J. *Grant's Dissector*, 17th ed.; LWW: Philadelphia, PA, USA, 2020.
17. Balta, J.Y.; Twomey, M.; Moloney, F.; Duggan, O.; Murphy, K.P.; O'Connor, O.J.; Cronin, M.; Cryan, J.F.; Maher, M.M.; O'Mahony, S.M. A comparison of embalming fluids on the structures and properties of tissue in human cadavers. *Anat. Histol. Embryol.* **2019**, *48*, 64–73. [[CrossRef](#)] [[PubMed](#)]
18. Gulati, A.; Knott, P.D.; Seth, R. Sex-Related Characteristics of the Face. *Otolaryngol. Clin. North Am.* **2022**, *55*, 775–783. [[CrossRef](#)]
19. Peters, F.; Mücke, M.; Möhlhenrich, S.C.; Bock, A.; Stromps, J.P.; Kniha, K.; Hölzle, F.; Modabber, A. Esthetic outcome after nasal reconstruction with paramedian forehead flap and bilobed flap. *J. Plast. Reconstr. Aesthetic Surg.* **2021**, *74*, 740–746. [[CrossRef](#)] [[PubMed](#)]
20. Sahu, R.K.; Acharya, S.; Midya, M.; Chakraborty, S.S. Expanded Paramedian Forehead Flap for Nasal Reconstruction Following Congenital Nevus Excision. *Plast. Aesthetic Nurs.* **2022**, *42*, 163–166. [[CrossRef](#)]
21. Rajan, S.; Akhtar, N.; Kumar, V.; Gupta, S.; Misra, S.; Chaturvedi, A.; Chaudhary, S.; Suryavanshi, P. Paramedian forehead flap reconstruction for skin tumors involving central subunit of face: An analysis of 37 cases. *J. Oral Biol. Craniofacial Res.* **2020**, *10*, 764–767. [[CrossRef](#)] [[PubMed](#)]
22. Gupta, R.; John, J.; Hart, J.; Chaiyasate, K. Medial Canthus Reconstruction with the Paramedian Forehead Flap. *Plast. Reconstr. Surg. Glob. Open* **2022**, *10*, e4419. [[CrossRef](#)]

23. Immaneni, S.; Harvey, D.T.; Delgado, F. Reuse of the paramedian forehead flap pedicle: A case report. *SAGE Open Med. Case Rep.* **2023**, *11*, 2050313X231160913. [[CrossRef](#)]
24. Tripathy, S.; Garg, A.; John, J.R.; Sharma, R.K. Use of Modified Islanded Paramedian Forehead Flap for Complex Periocular Facial Reconstruction. *J. Craniofac. Surg.* **2019**, *30*, e117–e119. [[CrossRef](#)]
25. Itani, Y.; Yotsuyanagi, T.; Yamauchi, M.; Sugai, A.; Kato, S.; Yamashita, K.; Isogai, N. The Laterally Extended Paramedian Forehead Flap for Nasal Reconstruction: The Delay Technique Revisited. *Plast. Reconstr. Surg. Glob. Open* **2020**, *8*, e2871. [[CrossRef](#)] [[PubMed](#)]
26. Lo Torto, F.; Redi, U.; Cigna, E.; Losco, L.; Marcasciano, M.; Casella, D.; Ciudad, P.; Ribuffo, D. Nasal Reconstruction With Two Stages Versus Three Stages Forehead Fap: What is Better for Patients With High Vascular Risk? *J. Craniofacial Surg.* **2020**, *31*, e57–e60. [[CrossRef](#)] [[PubMed](#)]
27. Little, S.C.; Hughley, B.B.; Park, S.S. Complications with forehead flaps in nasal reconstruction. *Laryngoscope* **2009**, *119*, 1093–1099. [[CrossRef](#)] [[PubMed](#)]
28. Chakraborty, S.S.; Goel, A.D.; Sahu, R.K.; Midya, M.; Acharya, S.; Shakrawal, N. Effectiveness of Nasolabial Flap Versus Paramedian Forehead Flap for Nasal Reconstruction: A Systematic Review and Meta-analysis. *Aesthetic Plast. Surg.* **2023**, *47*, 313–329. [[CrossRef](#)]
29. Chen, C.L.; Most, S.P.; Branham, G.H.; Spataro, E.A. Postoperative Complications of Paramedian Forehead Flap Reconstruction. *JAMA Facial Plast. Surg.* **2019**, *21*, 298–304. [[CrossRef](#)]
30. Eskiizmir, G.; Tanyeri Toker, G.; Ozgur, E.; Tarhan, S.; Cengiz Ozyurt, B. Hemodynamic Changes in Paramedian Forehead Flap. *J. Craniofacial Surg.* **2018**, *29*, 159–162. [[CrossRef](#)]
31. Society, A.C. Cancer Facts & Figures 2023. Available online: <https://www.cancer.org/research/cancer-facts-statistics/all-cancer-facts-figures/2023-cancer-facts-figures.html> (accessed on 1 December 2023).

**Disclaimer/Publisher’s Note:** The statements, opinions and data contained in all publications are solely those of the individual author(s) and contributor(s) and not of MDPI and/or the editor(s). MDPI and/or the editor(s) disclaim responsibility for any injury to people or property resulting from any ideas, methods, instructions or products referred to in the content.